## Werk

**Jahr:** 1975
**Kollektion:** fid.geo
**Signatur:** 8 Z NAT 2148:41
**Digitalisiert:** Niedersächsische Staats- und Universitätsbibliothek Göttingen
**Werk Id:** PPN1015067948_0041
**PURL:** http://resolver.sub.uni-goettingen.de/purl?PPN1015067948_0041

**LOG Id:** LOG_0059
**LOG Titel:** A seismic reflection method for solving engineering problems
**LOG Typ:** article

## Übergeordnetes Werk

**Werk Id:** PPN1015067948
**PURL:** http://resolver.sub.uni-goettingen.de/purl?PPN1015067948
**OPAC:** http://opac.sub.uni-goettingen.de/DB=1/PPN?PPN=1015067948



## Contact

Niedersächsische Staats- und Universitätsbibliothek Göttingen
Georg-August-Universität Göttingen
Platz der Göttinger Sieben 1
37073 Göttingen
Germany
Email: gdz@sub.uni-goettingen.de

J. Geophys. 41, 367–384, 1975

# A Seismic Reflection Method for Solving Engineering Problems

R. Schepers

Institut für Geophysik der Ruhr-Universität Bochum

Received November 15, 1974

*Abstract.* In this paper a seismic reflection technique capable of resolving thin near surface layers is described. The theoretical discussion is accompanied by a case history demonstrating the identification of four reflections within a time interval of 15 ms corresponding to a total depth of 8 m.

Body waves are generated by means of a thumber on the bottom of a small borehole thus suppressing the coherent noise in the reflection seismograms (*S*-waves and surface waves). The described digital recording system provides efficient suppression of the incoherent noise by means of an on-line averaging process. Its high dynamic range has enabled a successful application of processing techniques with the following features: The deconvolution of one-channel seismograms and the suppression of multiples are achieved by means of homomorphic filtering. Equally the wavelet emitted by the seismic source can be separated from an one-channel seismogram by means of homomorphic filtering. This wavelet can be used to yield the deconvolution of multi-channel seismograms by means of optimum inverse filtering.

*Key words*: Engineering Seismics – Reflection Method – Seismic Field Technique – Noise Suppression – Homomorphic Filtering – Deconvolution – Suppression of Multiples.

## *1. Introduction*

In engineering geophysics seismic measurements can help to determine the physical and lithological properties of the uppermost part of the crust including depths of a few meters to at least 100 meters. These seismic measurements are generally carried out for civil engineering purposes, for the location of subsurface cavities and for hydrogeological and rock mechanical investigations. In case of delineating interfaces or locating faults and cavities these investigations are labelled 'structural'.

Until now for structural investigations the seismic refraction technique is commonly used. Certainly the refraction technique provides not only the depths of the different interfaces but also the velocities in each of the layers yet there are some cases where it fails:

i) The length of the geophone spread has to be about 5 times greater than the depth of the deepest refractor. Hence measurements within urban areas are difficult or rather impossible. Moreover, the interpretation of refraction measurements carried out by means of long geophone spreads leads to rough models of the subsurface or, supposing the geological situation is complicated, completely fails. This problem can partly be overcome by shooting overlapping profiles.

ii) A necessary assumption for the use of the refraction technique are velocities increasing with depth. If this assumption is not valid the interpretation will be erroneous to a great extent.

iii) Supposing only first arrivals are used for interpretation 'overshooting' of layers can occur (blind zone problem).

iv) Locating a subsurface cavity by means of the refraction technique may only be possible for the special case the refractor intersecting the cavity or passing closely underneath.

There are few attempts to make use of the seismic reflection technique (Meidav, 1969; Stoll, 1971) though it has many advantages and has proven to be a powerful tool in exploration geophysics. The reflection technique can be applied to all the problems mentioned above. This is partly due to the short geophone spread used in the reflection technique. A further advantage is the more detailed image yielded by means of the seismic reflection technique.

The difficulties in using the reflection technique for problems of engineering geophysics can be described as follows:

In exploration geophysics both the depth to the deepest reflector and the thickness of the thinnest layer are about 40 times greater than in engineering geophysics. Assuming the same layer thickness-to-wavelength ratio for both exploration and engineering geophysics means for the latter case the use of signals with dominant frequencies of about 1000 Hz. Supposing the use of a hammer or a thumber as source of the seismic signal the mentioned high frequencies cannot be produced in soil. As our experiments with different types of a hammer or a thumber and an electrical sparker buried in a water-filled borehole showed seismic signals received in a distance of 2 meters to the source contained frequencies in the range of 50 Hz to 800 Hz with dominant frequencies about 150 Hz. Furthermore the duration of the source pulses came to about 15 ms.

For very many cases this means that the two-way traveltime of the seismic waves concerning the near surface layers is shorter than the duration of the source pulse. Let us e.g. assume a depth of 50 meters for the deepest reflector and a spread length of 25 meters we then find all reflected *P*- and *S*-waves recorded within a time of 50 to 100 ms depending on the velocity distribution. Hence a reflection technique that takes into account only *P*-wave arrivals has to solve three problems. It is necessary:

i) to suppress the unwanted parts of the seismic signal, e.g. the arrivals of *S*-waves and surface-waves,

ii) to compress the source pulse,

iii) to be able to distinguish primaries from multiples.

The field technique and the digital recording facilities described in the first part of this paper provide an efficient tool for suppressing unwanted seismic signals. The second part of this paper describes a digital process for the deconvolution of the near-surface reflection seismograms and the suppression of multiples. This is illustrated by a case history at the end of each chapter.

## *2. Field Technique*

### 2.1. The Digital Recording System

Among all possible processes of signal enhancement in near-surface reflection seismic the application of a deconvolution filter is essential. Provided the seismic signal has a broad frequency range and the signal-to-noise ratio is high this filter will

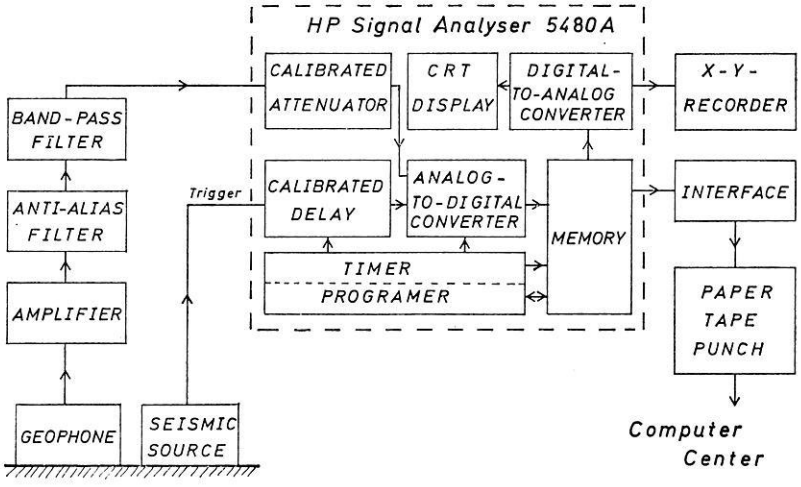


Fig. 1. Block diagram of the seismic recording system

be most effective. Consequently a highly resolved record is an essential condition for a broad frequency range used for the deconvolution process. Since no qualified recording system for near-surface reflection measurements is available Rüter[1] and Schepers designed a digital recording system which embodies further advantages beyond the great dynamic range of its stored data. This recording system improves the signal-to-noise ratio by means of an on-line averaging process. Fig. 1 shows a block diagram of the system. The recorded seismic signal is converted to digital data and stored in a magnetic core memory. Part of the hardware yields the averaging of repetitive signals and hence improves the signal-to-noise ratio and the resolution of the analogue-to-digital conversion. The resolution due to one process cycle is 54 dB. Doubling the number of process cycles improves the resolution for 6 dB and the signal-to-noise ratio for 3 dB. Hence the dynamic range of the digitally stored data is improved for 3 dB. Performing 16 process cycles means a dynamic range of 66 dB and an improvement of the signal-to-noise ratio for 12 dB. The digital-to-analogue converter provides a continuous display of the data on a CRT without flickering. So a signal improvement can be visually controlled. This holds during the run-down process of a cycle too. As the averaging process is executed in real-time this recording system provides an immense data reduction.

The memory of the used signal analyser allows the storage of 1000 24-bit words. It can be divided into quarters so that four different input signals can be processed simultaneously. In this case the minimum sampling rate of the used apparatus is 0.04 ms corresponding to a Nyquist frequency of 12.5 kHz being sufficient even for measurements in solid rock.

The final data can be plotted on an X-Y-recorder and punched on a tape. Further processing of the data is carried out in a computer center. In the final stage of system

1 Dipl. Geophys. H. Rüter, Institut für Geophysik, Schwingungs- und Schalltechnik der Westfälischen Berggewerkschaftskasse, Bochum, Herner Straße 45.

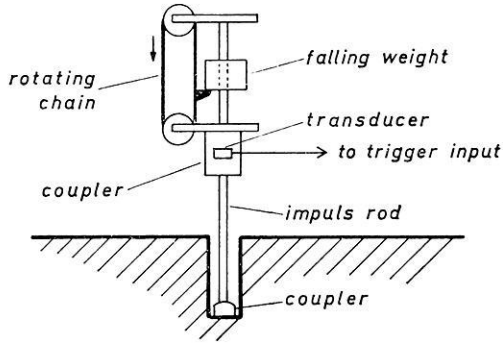


Fig. 2. Scheme of the seismic source

development all processes of signal enhancement should be done immediately in the field by means of a processor.

## 2.2. The Seismic Source

A thumber was designed to be employed either in vertical boreholes or on the surface. Fig. 2 shows a scheme of its construction. An electric motor drives a rotating chain lifting the weight. The dropping weight strikes a coupler on top of a rod causing a displacement of another coupler on the bottom of the borehole. Hence the second coupler emits body waves. As we want to produce an averaged seismic signal based on several weight-drops a reliable trigger signal is essential. After failure of many experiments we came to using a piezoelectric transducer shaped like a disc and cemented into the first coupler on top of the rod. The weight drop generated compressional wave in this coupler gives rise to a trigger pulse having an amplitude of roughly 1 V and a rise time of a few microseconds. The repetition rate of the weight drops is variable from 1 Hz to 0.2 Hz. The shape of the seismic pulse emitted by this source is reproduced very well.

## 2.3. Case History

*2.3.1. The Test Site.* Our first field experiments have taken place in the neighbourhood of the Bochum University within the 'Ruhrtal'. We generally shall refer to this site with the abbreviation 'BRT'. There are several arguments for choosing BRT as test site:

i) A few boreholes exist being drilled in connection with a survey for drinking-water. Hence the lithological sequence at some points of the area is well known. The data supplied by boreholes are given in Table 1.

ii) From the data given in Table 1 we can infer a sharp separation of the different layers and fairly flat reflectors.

iii) There exist three reflectors within a depth of 8 m. The two-way traveltime of *P*-waves within the different layers comes to only 5 ms on an average. However if the reflection technique will successfully be applied within the scope of engineering geophysics it should be possible to resolve reflections separated only a few milliseconds.

Table 1. Data supplied by boreholes

| lithology | BRT1 | BRT2 | BRT3 |
|---|---|---|---|
| sandy clay | 0. −1.2 m | 0. −2.0 m | 0. −1.6 m |
| sand with fine gravel (dry) | | | 1.6 −3.9 m |
| sand with fine gravel (wet) | | | 3.9 −6.1 m |
| coarse gravel (dry) | 1.2 −3.2 m | 2.0−4.1 m | |
| coarse gravel (wet) | 3.2 −8.1 m | 4.1−7.0 m | 6.1 −8.5 m |
| bedrock (shale, sandstone) | 8.1 m− | | 8.5 m− |

Table 2. *P*-wave velocities derived from refraction surveys

| lithology | profile 1, 3 (BRT1,2) | profile 2 | profile 4, 6 | profile 5 (BRT3) |
|---|---|---|---|---|
| sandy clay | 430 m/s | 400 m/s | 360 m/s | 390 m/s |
| sand with fine gravel (dry) | | | 690 m/s | |
| sand with fine gravel (wet) | | | | 1150 m/s |
| coarse gravel (dry) | | 850 m/s | | |
| coarse gravel (wet) | 1670 m/s | | | |
| bedrock (shale, sandstone) | 3100 m/s | 3200 m/s | 3050 m/s | 2950 m/s |

On BRT test site six refraction surveys were carried out to yield information about the *P*-wave velocities in the different layers. The layers identified by means of drilling holes (c.f. Table 1) and their corresponding velocities are listed in Table 2. The results indicate that all refraction surveys contain the effect of 'overshooting' one layer causing an erroneous calculation of the depth to the bedrock. So e.g. a straigthforward interpretation of the refraction data on site BRT1 results in a depth of 6.3 m to the bedrock instead of 8.1 m derived from the drilling survey.

*2.3.2. Field Procedure and Results.* For a model corresponding to site BRT1 theoretical traveltime curves were computed. Fig. 3 depicts the traveltime curves of the direct *P*- and *S*-wave, the reflected *P*-primaries and a surface wave having a velocity of 230 m/s. Supposing the length of the source pulse comes to at least 10 ms, the traveltime curves in Fig. 3 indicate that there is no favorable shot-to-geophone distance yielding a separation of the reflected primaries from one another or from other signal generated arrivals. For small shot-to-geophone distances the direct *P*-wave and the *S*-waves disturb the reflection arrivals. At a distance of 5 m the traveltime curves of the first two reflection arrivals cross over and refraction arrivals begin to emerge.

Supposing very shallow reflectors efficient attenuation of the surface wave seems to be important producing interpretable seismograms. Our field experiments have shown that a seismic source coupled to the soil on the bottom of a shallow borehole as described above has the advantage of diminishing the amplitude of the surface wave to a great extent. E.g. a reflection seismogram section containing 30 traces is given in Fig. 4. The source was at a depth of 2 m just on top of the gravel (c.f. Table 2). The geophones have been placed on the surface with distances between 0.2 m and 6 m to the epicentre. As site BRT2 lies 30 m apart a motor-road the on-line

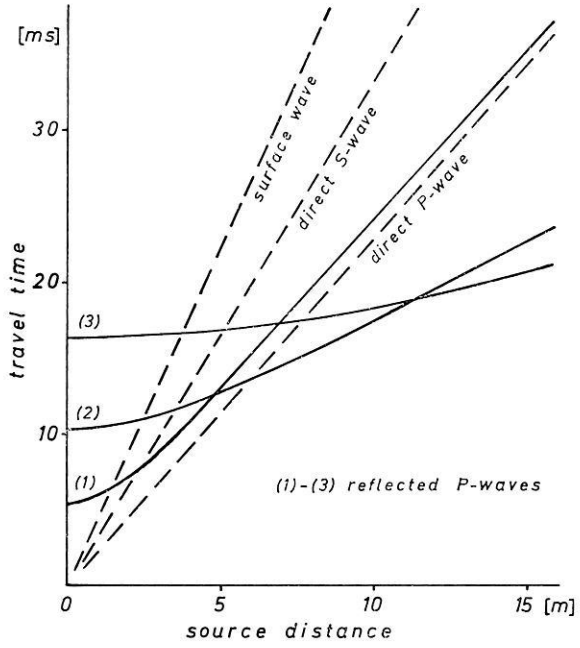


Fig. 3. Theoretical traveltime curves for site BRT1

averaging process of the recording system was used to suppress the traffic generated noise. As the amplitude of the surface wave in Fig. 4 is low for distances less than 3 m we can clearly correlate two reflected arrivals at different shot-to-geophone distances. The one found at distances between 0.2 m and 2.0 m is due to the *P*-wave reflected by the ground water surface; the other one existing at distances between 1.6 m and 3.8 m is due to the reflection by the bedrock. Though the reflected arrivals can clearly be separated the determination of the traveltime differences between the direct arrival and the reflected ones — being essential for computing layer thickness — is difficult. Despite of this traveltime estimations for the two reflected pulses agree well with the traveltimes computed from the available data at site BRT2.

Summarizing the results of our measurements we can say: Unprocessed reflection seismograms with clearly distinguishable reflection arrivals can be obtained even in cases where the two-way traveltime comes to only few milliseconds. Yet data processing seems to be necessary improving the resolution and making an exact interpretation possible.

### *3. Deconvolution and the Suppression of Multiples*

Using a weight-drop on the bottom of a borehole is advantageous in so far as a geophone placed close to the epicentre receives only *P*-waves travelled upwards. (This statement is exactly valid in case of horizontally layered sequences). Hence the output of this geophone is a comparatively simple seismic signal and we expect signal enhancement processes to be less complicated and in due course more effective. E.g.

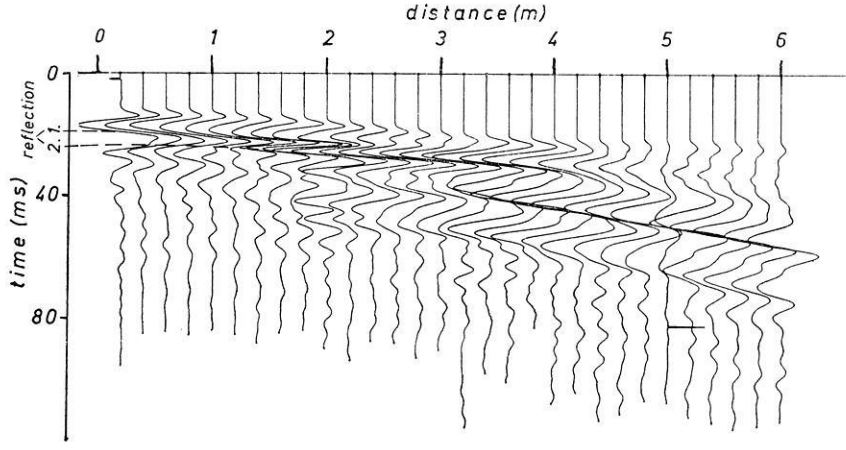


Fig. 4. Reflection seismogram recorded at site BRT2

in Fig. 4 the trace at the distance of 0.2 m should only contain vertically travelled *P*- waves. For the main part of this chapter we will discuss how to filter such one-channel reflection seismograms. The assumptions the filter design is based on are given in the first part of this chapter.

### 3.1. Synthetic Seismograms

Assuming the behaviour of the earth is describable as a linear system a seismic signal generally represents the convolution of a wavelet representing the source pulse with the unit impulse response of an elastic earth model. Furthermore perfect elasticity yields linear systems containing constant parameters. Given the case of vertically travelling *P*- waves in a horizontally layered subsurface computer programs for numerical solutions of the unit impulse response are simple (Robinson,1967; Schepers, 1972). Synthetic seismograms for such a model of the lithological sequence are derived from the convolution of a wavelet with the unit impulse response.

The computation of the synthetic seismogram is entirely based on plane-wave theory yet a correction of the spherical divergence of the wavefront can easily be included into the program. For practical applications we have to consider additional noise. Hence the synthetic seismogram $s(n)$ reads:

$$s(n) = w(n) * r(n) + v(n) * u(n)$$

where $w(n)$ represents the seismic wavelet, $r(n)$ represents the unit impulse response, $u(n)$ represents a white time series, and $v(n)$ represents the noise wavelet. It ought to be stressed that this representation of a seismic signal is not unique. Yet its usefulness will be appreciated by the degree of success in interpretating field seismograms. Two processes of signal enhancement shall be considered:

i) The separation of the unit impulse response from the wavelet, commonly termed as deconvolution.

ii) The suppression of multiples.

### 3.2. Homomorphic Deconvolution

Deconvolution can be performed by inverse filtering or by Wiener filtering, provided the shape of the seismic wavelet to be removed is known or the wavelet is a minimum-delay one and the unit impulse response of the subsurface layering is a white series (this means the autocorrelation $\Phi(\tau)=0$ except for $\tau=0$) (Robinson, 1967; Robinson and Treitel, 1967). Using predictive deconvolution (Peacock and Treitel, 1969) the only assumption is the unit impulse response to be a white series.

As in most cases we have at least one thin surface layer and hence the individual wavelets will overlap to a great extent we cannot expect to know the shape of the wavelet in near-surface reflection work. This is demonstrated by the reflection seismogram in Fig. 4. On the other hand the unit impulse response is far from being a white series because in near-surface reflection surveys we typically find a few reflectors with great reflection coefficients. Together with the reflection coefficient equal to 1 at the surface this leads to strong multiples. E.g. in the unit impulse response of Fig. 7 the only arrivals to be regarded as random ones are the three primary arrivals. All other arrivals mainly shaping the unit impulse response are deterministic.

Oppenheim (1965) has formulated the general theory for the synthesis of nonlinear filters for signals which can be expressed as a convolution of components. Known as homomorphic filtering this method has been applied by Oppenheim, Schafer and Stockham (1968) to image enhancement, echo removal and speech waveform processing. Ulrych (1971, 1972) has presented the application of homomorphic filters for the recovery of the seismic wavelet out of a time series formed by the convolution of this wavelet with a spike series. He used this method known as homomorphic deconvolution separating the seismic wavelet in earthquake seismograms.

Concerning our problem homomorphic filters have the considerable advantage that no assumption about the unit impulse response and the delay properties of the wavelet needs to be made. The theory and the principles of applying homomorphic filters have fully been dealt with by Oppenheim (1965) and Oppenheim *et al.* (1968) and considerations concerning their realisation on digital computers are given by Oppenheim *et al.* (1968) and Ulrych (1971). Here only a brief summary of the principles of homomorphic filtering shall be given.

The general principle of homomorphic filtering corresponds to transforming the original problem to a space where the components are added, and — after linear filtering — transforming the results back to the original space of inputs. According to this principle a homomorphic filter represents a cascade of three systems as shown in Fig. 5. The system $D$ in Fig. 5 called the characteristic system is a nonlinear system transforming the input sequence $x(n)$ from a convolutional space to an additive space. The function $\hat{x}(n)$ being the output of the system $D$ and the input of the system $L$ is called the complex cepstrum. The system $L$ is a linear system. The system $D^{-1}$ shown in Fig. 5 is the inverse system to $D$, $D^{-1}$ transforms the output $\hat{y}(n)$ of the

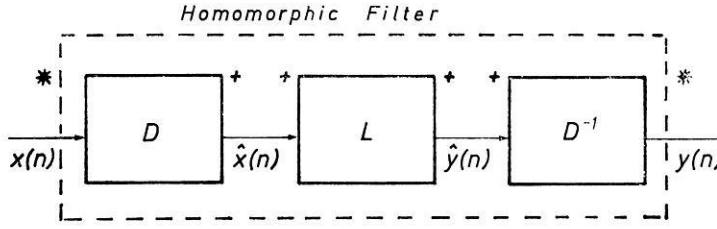


Fig. 5. Representation of homomorphic filtering as a cascade of three systems

system $L$ from an additive space into a convolutional space. The characteristic system $D$ remains the same for all filtering problems, only the linear system $L$ has to be adapted. We find the system $D$ successively consisting of the $z$-transform, the natural logarithm and the inverse $z$-transform. The system $D^{-1}$ successively consists of the $z$-transform, the exponential function and the inverse $z$-transform.

Practical applications involve the use of finite time series. Each finite time series $s(n)$ is to be considered as the convolution of a minimum delay time series $s_1(n)$ with a maximum delay time series $s_2(n)$

$$s(n) = s_1(n) * s_2(n)$$

The complex cepstrum $\hat{s}_1(n)$ of $s_1(n)$ is zero for $n<0$ and the complex cepstrum $\hat{s}_2(n)$ of $s_2(n)$ is zero for $n>0$ (Oppenheim *et al.*, 1968; Schepers, 1972). Hence follows that the maximum delay and the minimum delay components of a signal are completely separated in the complex cepstrum.

How the actual separation of convolved components is carried out by the system $L$ of Fig. 5, is illustrated by means of a simple example in Fig. 6. Time series (1) in Fig. 6 consists of two spikes separated only by four samples. This spike series represents a minimum delay time series whereas the wavelet (2) is a mixed delay one. The complex cepstrum (4) of the spike series (1) only contains non-vanishing amplitudes for $n \geqslant 4$. The value $n=4$ is due to the time difference between the two spikes in time series (1). On the other hand the main contribution of the wavelet (2) to the complex cepstrum (5) consists of values in the neighbourhood of $n=0$ and the amplitudes of the complex cepstrum decrease rapidly with increasing $n$. The system $L$ separating the two components — spike series and wavelet — of time series (3) from the complex cepstrum (6) simply consists of multiplying the complex cepstrum (6) with two rectangular time windows $I$ and $W$ as indicated in Fig. 6. The two time windows are fully defined by the time $t_c$ stating the latest time of the window $W$ and the first time of the window $I$. Furtheron the time $t_c$ shall be labelled 'cut-off time'.

In our example of Fig. 6 we have chosen a cut-off time $t_c = 3 \cdot \Delta t$ for separating the wavelet and the spike series. The outputs of the two different systems $L$ are transformed back to the time domain by the system $D^{-1}$. The results are shown in Fig. 6. As some contribution of the wavelet (2) to the complex cepstrum (3) occurs for values $n \geqslant 4$ time series (7) does not reproduce perfectly the wavelet (2). Yet time series (8) is very much similar to the spike series (1).

Though the example given in Fig. 6 is simple the reflection response of the subsurface may be a very complex spike series. Nevertheless the wavelet $w(n)$ and the

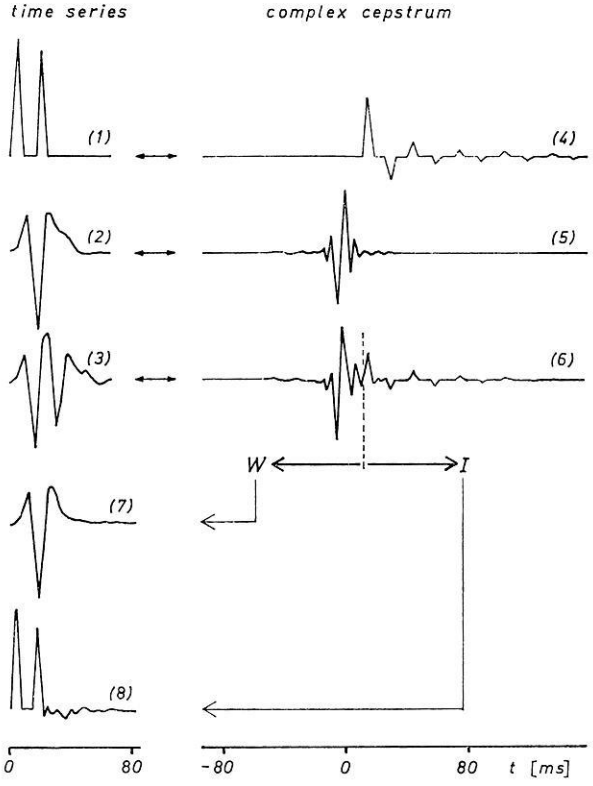


Fig. 6. The concept of the complex cepstrum as applied to homomorphic deconvolution. (1) impulse series with one echo, (2) wavelet, (3) convolution of (1) and (3), (4) (5) (6) complex cepstra of (1) (2) (3), (7) wavelet reconstructed from part W of (6), (8) impulse series reconstructed from part I of (6)

unit impulse response $i(n)$ of a real seismogram $x(n) = w(n) * i(n)$ are separable in the same way as illustrated above. Necessary conditions are the series $i(n)$ to be a minimum delay one and the time difference between the first two spikes to be sufficently great. The first condition can easily be fullfilled in seismic reflection surveys as spherical divergence causes the unit impulse response to be minimum delay in most cases. If this is not true the series $i(n)$ can be made into a minimum delay one by exponential weighting (Ulrych, 1971). The second assumption is more severe, because the lithological sequence often contains a thin surface layer with a reflection time of a few milliseconds. In these cases the separation of the wavelet may be impossible, but the identification of deeper reflection is not affected at all.

### 3.3. Suppression of Multiples

In the case of one layer over a halfspace the $z$-transform of the unit impulse response $r(n)$ can be written as follows (Robinson, 1967):

$$R(z) = (1 + cz^{-1}) / (1 - cz^{-1}) \tag{1}$$

where $c$ is the reflection coefficient between the layer and the halfspace, and the two-way traveltime through the layer has been assumed to be one sampling rate. To compute the complex cepstrum $\hat{r}(n)$ of $r(n)$ we have to take the natural logarithm of $R(z)$:

$$\begin{aligned}
\ln R(z) &= \ln(1 + cz^{-1}) - \ln(1 - cz^{-1}) \\
&= cz^{-1} - (c^2/2)z^{-2} + (c^3/3)z^{-3} - (c^4/4)z^{-4} + (c^5/5)z^{-5} + \ldots \\
&+ cz^{-1} + (c^2/2)z^{-2} + (c^3/3)z^{-3} + (c^4/4)z^{-4} + (c^5/5)z^{-5} + \ldots \\
&= 2cz^{-1} + 2(c^3/3)z^{-3} + 2(c^5/5)z^{-5} + \ldots
\end{aligned}$$

The complex cepstrum, therefore, is the time series $\hat{r}(n) = (0,\ 2c,\ 0,\ 2c^3/3,\ 0,\ 2c^5/5, \ldots)$ whereas the reflection response according to Eq. (1) is the time series $r(n) = (1,\ 2c,\ 2c^2,\ 2c^3,\ 2c^4,\ 2c^5, \ldots)$. Taking the complex cepstrum $\hat{r}(n)$ as the final result we find that in comparison with the series $r(n)$ the multiple events are suppressed to a great extent. The complex cepstrum $\hat{r}(n)$ essentially displays the primary reflection. A numerical example will illustrate this statement. Assuming $c = -0.5$ we find the two series

$$r(n) = (1.,\ -1.,\ 0.5,\ -0.25,\ 0.125,\ -0.0625, \ldots)$$
$$\hat{r}(n) = (0,\ -1,\ 0,\ -0.0833,\ 0,\ -0.0125, \ldots)$$

In the complex cepstrum the first multiple completely has vanished and the amplitude of the second multiple is one third of the amplitude of the second multiple in the unit impulse response.

Further analytical computations concerning the multilayer case are given by Schepers (1972). It turns out that the complex cepstrum as final result instead of the deconvolved signal can give a good image of the layered subsurface. Yet it ought to be stressed that considerable errors can occur if the reflection coefficient does vary too much with depth.

The efficiency of suppressing multiples by homomorphic filtering will be illustrated by a synthetic example. For the example in Fig. 7 a model was chosen of two thin surface layers producing strong multiples as the unit impulse response (2) in Fig. 7 demonstrates. A deep interface with a considerable smaller reflection coefficient is masked by these multiples. Time series (4) is the complex cepstrum of the seismogram (3) for values of $t \geqslant 10$ ms. The deconvolution — no noise has been added in this synthetic seismogram — is perfect and the suppression of the multiples is satisfactory. The third reflection can be identified clearly. The signal enhancement yielded by means of homomorphic filtering can be concluded from the input signal (3) in Fig. 7 and from comparing the output signal (4) with the wanted signal (1).

From this it follows that the use of the complex cepstrum instead of the unit impulse response leads directly to a good image of the subsurface. Besides computing time is saved and as long as we do not intend to extract the shape of the wavelet from the seismogram the choice of the cut-off time is not critical, because the cut-off time only determines the two-way traveltime to the first reflector we are interested in.

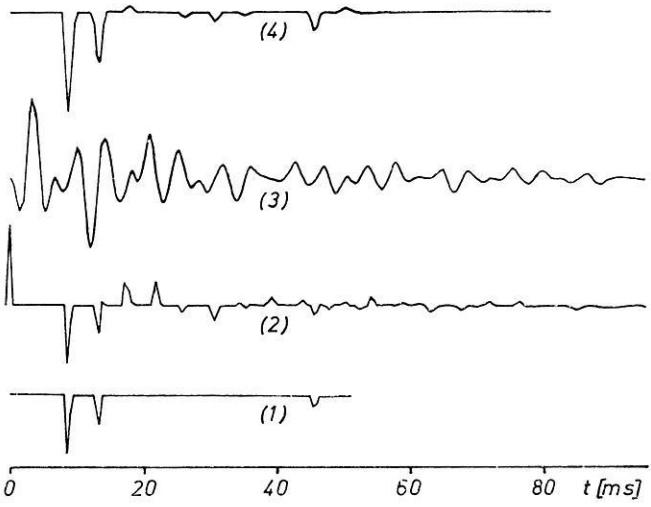


Fig. 7. Suppression of multiples. (1) series of primary reflections, (2) unit impulse response, (3) synthetic seismogram, (4) complex cepstrum of (3) for $t \geqslant 10$ ms

### 3.4. Computational Considerations

There are some important considerations in the computation of the complex cepstrum fully described by Oppenheim *et al.* (1968) and Ulrych (1971). So only those aspects shall be emphasized that have not been discussed so far.

We assume that the seismogram can be written in the form $s(n) = w(n) * r(n) + u(n)$ where $u(n)$ is a white series. It is preferable to use the Fast Fourier Transform for the numerical computation of the complex cepstrum instead of the $z$-transform (Oppenheim *et al.*, 1968). The natural logarithm of the complex spectrum can be computed via the amplitude and the phase spectrum. Special care has to be taken in the computation of the amplitude and phase spectra. This means:

i) A noisy signal has to be considered as an infinite time series. Before processing, therefore, the seismogram is multiplied with a 'hamming' window having a length of 2—3 times the two-way traveltime to the deepest reflector. Multiplying a time series with a window corresponds to a filter process in the frequency domain.

The curve (1) in Fig. 8 is the amplitude spectrum of a unit impulse response $r(n)$. The amplitude spectrum (2) is computed from a seismogram $s(n) = r(n) * w(n)$. The amplitude spectrum (3) of a seismogram $s(n) = r(n) * w(n) + u(n)$ is computed without using a time window. The result yielded by multiplying with a hamming window is the amplitude spectrum (4), which is an acceptable approximation of the noise-free spectrum (2).

ii) If noise is present difficulties will arise for the computation of the phase spectrum. The phase spectrum (7) of the noisy seismogram in Fig. 8 shows great deviations with respect to the phase spectrum (6). Considering the phase curves as time series we can classify the deviations as low-frequency noise that can be filtered out by high pass filter.

The result after applying this process is the phase spectrum (8) in Fig. 8. The low-frequency component of the phase spectrum (6) of the seismic wavelet is also filtered

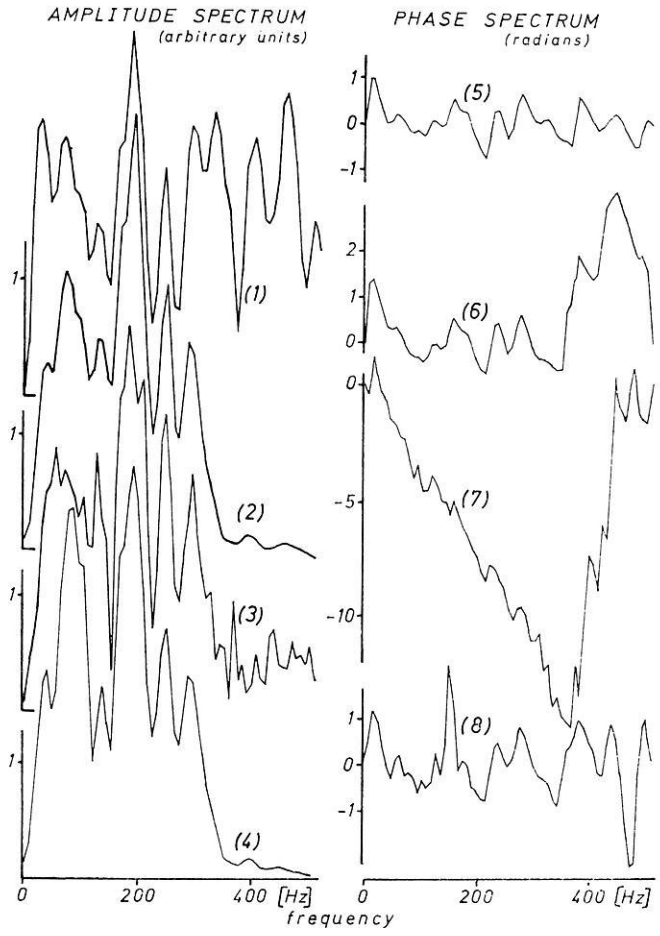


Fig. 8. The computation of the amplitude and the phase spectrum. (1) amplitude spectrum of the unit impulse response of the model shown in Fig. 10, (2) amplitude spectrum of the synthetic seismogram (1) in Fig. 10, (3) amplitude spectrum of the synthetic seismogram (2) in Fig. 10, (4) amplitude spectrum gained by filtering of the amplitude spectrum (3), (5) (6) (7) phase spectra corresponding to (1) (2) (3), (8) phase spectrum gained by filtering of the phase spectrum (7)

out and the phase spectrum (8) resembles more the phase spectrum (5) of the unit impulse response than the phase spectrum (6) of the seismogram. This means: If we want to extract the shape of the wavelet from the seismogram we must use the original phase curve.

### 3.5. Application of the Processing Technique to One-Channel Seismograms

Using a source at the bottom of a borehole we have to distinguish between reflections due to energy being emitted upwards and downwards. This situation is depicted in Fig. 9 for a two-layer case: The first multiple reflection from the first interface (3) arrives at the surface after the primary reflection from the second inter-

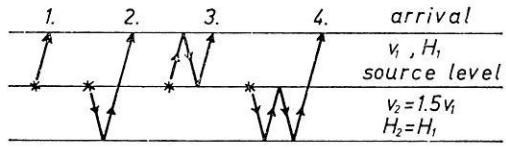


Fig. 9. The sequence of reflection arrivals for a source at the bottom of a borehole

face (2). This means reflections from deeper interfaces can be disturbed. Concerning the Ruhrtal test site we may expect the two-way traveltime through the first layer to be greater than the two-way traveltime from the source to the deepest reflector. Hence, the interpretation will be simple. It is important to note that this will not be true in most cases. Preliminary considerations must be made about the optimal depth of the source. Computation of the unit impulse response can help to solve this problem.

Assuming a source at the bottom of a borehole homomorphic filtering of synthetic seismograms for BRT was carried out to decide whether the complex cepstrum can be a good approximation to the series of the primary reflections. The results are shown in Fig. 10. The source was assumed to be 2 m deep just on top of the third layer. The time series (5) contains the primary reflections. They are labelled by numbers corresponding to the interfaces causing the reflections. The reflections labelled 3, 4 and 5 are due to a wave initially travelling downward from the source. The wave initially travelling upwards is reflected at the surface before giving rise to the reflections 1 and 2. The wavelet (6) in Fig. 10 was used to establish the seismogram (1). The corresponding unit impulse response was corrected for spherical divergence. The seismogram (2) is the same as (1) except for additive noise $u(n) * v(n)$, where $u(n)$ is a white series and $v(n)$ is the wavelet (6) in Fig. 10. The signal-to-noise ratio amounts to 2. The complex cepstrum (3) of the seismogram (1) sufficiently reproduces the primary reflections. The reflections for traveltimes greater than 15 ms are suppressed by the filtering process. The complex cepstrum (4) of the noisy seismogram (2) is worst, but the three reflections from beneath the source can be identified. The wavelets (7) and (8) in Fig. 10 were separated by homomorphic filtering using a cut-off time of 4.5 ms. Only the wavelet (7) is an acceptable approximation of the original wavelet (6). Considering the unfavourable signal-to-noise ratio of 2 this result is not unexpected.

Between site BRT2 and BRT3 8 one-channel reflection seismograms were recorded. The source was on the bottom of a borehole at a depth varying from 2.1 m to 2.7 m. To be sure that only vertically travelled *P*-waves are recorded one geophone — GEO SPACE GSC-11D — was placed at the surface directly besides the borehole. Each recorded seismogram represents the averaged signal of 16 weight drops. The sampling rate was 0.6 ms corresponding to a Nyquist frequency of 835 Hz. The results obtained by processing of these field seismograms are shown in Fig. 11. In the upper part of Fig. 11 the 8 complex cepstra of the field seismograms are plotted for times greater than 4.2 ms. Deflections of the traces to the left denote an increase of *P*-wave velocity. A multi-channel seismogram recorded at site BRT2 was already shown in Fig. 4. There were two reflections — the first from the ground water surface, the second from the bedrock — to be seen on this multi-channel

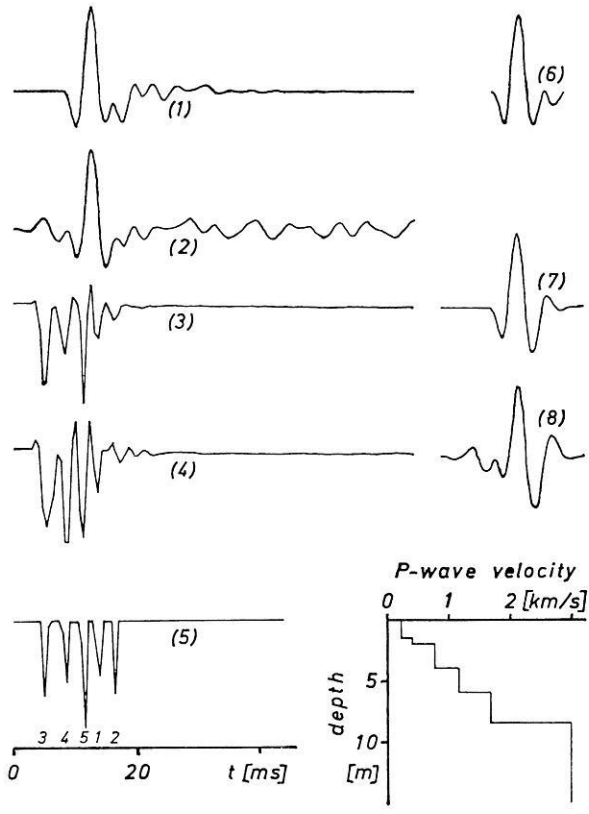


Fig. 10. Recovery of the primary reflections and the wavelet from synthetic seismograms for the Ruhrtal test site. (1) synthetic seismogram without noise, (2) synthetic seismogram with noise, (3) complex cepstrum of (1), (4) complex cepstrum of (2), (5) series of primary reflections, (6) wavelet used to construct the synthetic seismograms (1) and (2), (7) and (8) are the wavelets separated from synthetic seismogram (1) resp. (2) by homomorphic filtering

seismogram. These two reflections can be easily identified on the two traces for distances of 0. m and 20. m in Fig. 11. The other six traces in Fig. 11 display three reflections. The quality of the reflections is not satisfactory in all cases but it should be imagined the two-way traveltime between different reflections to be 5.5 ms at best. The interpretation of the 8 complex cepstra yielded the structure of the subsurface shown in the lower part of Fig. 11. The velocities the computation of the depth to the interfaces is based on are chosen according to the results of the refraction survey (Table 2). The data supplied by the borehole at site BRT3 (Table 1) is depicted in Fig. 11 for comparison.

The usefulness of the described processing technique depends on the assumptions given at the beginning of chapter 3. To test the validity of these assumptions for our field measurements synthetic seismograms were computed and compared with field seismograms. The velocity log for computing the unit impulse response was derived from the subsurface structure in the lower part of Fig. 11, the density log was estimated. The wavelet the unit impulse response was convolved with has been separated

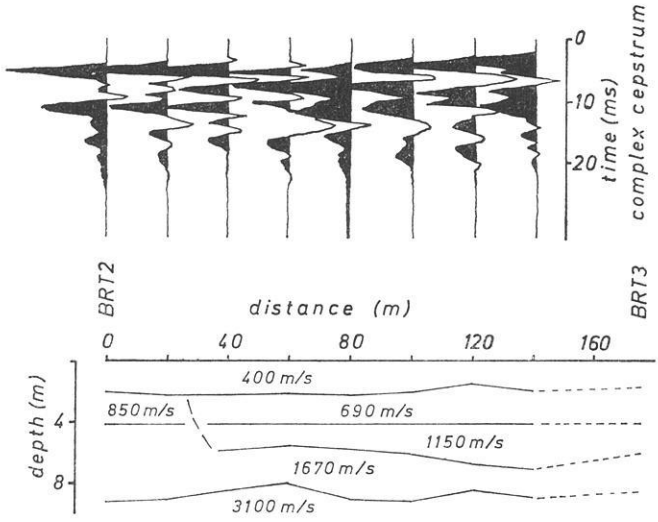


Fig. 11. The complex cepstra of field seismograms recorded between site BRT2 and BRT3, and the subsurface structure derived from the complex cepstra (the velocities are derived from refraction surveys)

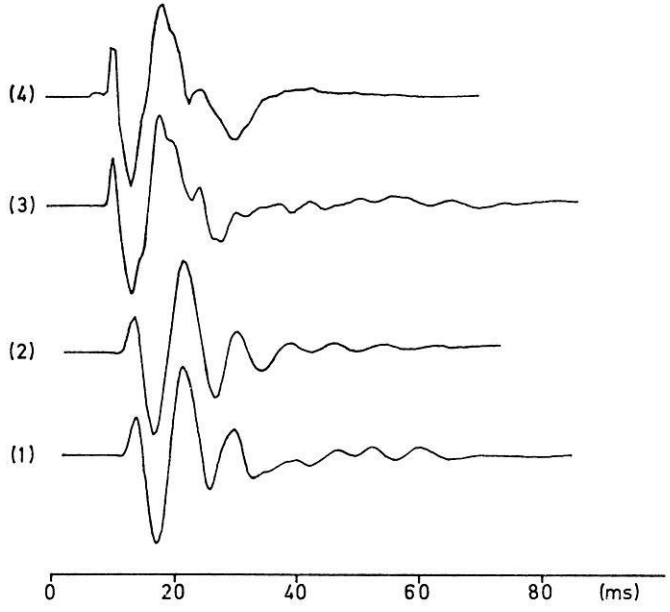


Fig. 12. Comparison of synthetic seismograms and field seismograms. (1) field seismogram for the distance of 0 m in Fig. 11, (2) synthetic seismogram for the distance of 0 m, (3) field seismogram for the distance of 40 m in Fig. 11, (4) synthetic seismogram for the distance of 40 m

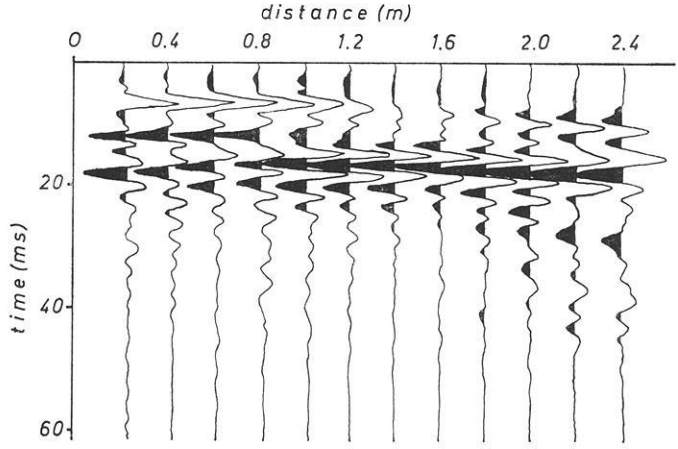


Fig. 13. Deconvolution of the first 12 traces of the seismograms shown in Fig. 4

from the corresponding field seismogram by homomorphic filtering. Two examples are given in Fig. 12: one for the case of two reflecting interfaces and one for the case of three reflecting interfaces beneath the source.

### 3.6. Improved Results for Multi-Channel Seismograms

As described in chapter 3.2. the wavelet emitted by the seismic source can be separated from the seismogram by homomorphic filtering. If the shape of the wavelet is known deconvolution can be achieved by optimum inverse filtering. One trace of the multi-channel seismogram shown in Fig. 4 was used to determine the wavelet of the emitted *P*-wave by homomorphic filtering. The optimum inverse operator of this wavelet was computed and each trace of the multi-channel seismogram was convolved with the inverse operator. The same procedure was carried out using different traces to determine the shape of the wavelet. The best result was obtained using the first trace recorded at the distance of 0.2 m.

E. g. Fig. 13 shows the results obtained by deconvolution of the first 12 traces of the seismogram shown in Fig. 4. The reflection from the ground water surface can be identified only on four traces, whereas the reflection from the bedrock correlates well for all 12 traces. Traces recorded at distances greater than 2.4 m are not shown as they increasingly display coherent noise. This is due to the arrival of S-waves and surface waves.

*Acknowledgements.* I am indebted to Prof. Dr. H. Baule for supporting this project. Thanks are expressed to Dipl.-Geoph. H. Rüter for stimulating discussions and to Prof. Dr. L. Dresen for critically reading the manuscript. The support of Dr. S. Freystätter for translating this paper is kindly appreciated. Part of this investigation has been carried out under DFG contract no. Dr 110/1.

*References*

Meidav, T.: Hammer reflection seismic in engineering geophysics. Geophysics *34*, 383–395, 1969

Oppenheim, A.V.: Superposition in a class of non-linear systems. Research Lab. of Electronics MIT, Tech. Rep. *432*, 1965

Oppenheim, A.V., Schafer, R.W., Stockham, T.G.: Nonlinear filtering of multiplied and convolved signals. Proc. IEEE *65*, 1264–1291, 1968

Peacock, K.L., Treitel, S.: Predictive deconvolution: theory and practise. Geophysics *34*, 155–169, 1969

Robinson, E.A.: Multichannel time series analysis with digital computer programs, 1rst ed. San Francisco: Holden-Day 1967

Robinson, E.A., Treitel, S.: Principles of Wiener filtering. Geophys. Prosp. *15*, 311–333, 1967

Schepers, R.: Bearbeitungsverfahren zur Bestimmung oberflächennaher Strukturen aus Einkanal-Reflexionsseismogrammen bei senkrechtem Einfall. Diss., University of Bochum, 1972. In: Berichte des Instituts für Geophysik der Ruhr-Universität Bochum, Nr. 2, Bochum 1972

Stoll, R.: Vibratorseismische Untersuchungen in realen Medien zur Nahortung und Kennwertbestimmung für ingenieurgeophysikalische Belange. Freiberger Forschungsh. *C 274*, 1971

Ulrych, T.J.: Application of homomorphic deconvolution to seismology. Geophysics *36*, 650–660, 1971

Ulrych, T.J.: Homomorphic deconvolution of some teleseismic events. Bull. Seism. Soc. Am. *62*, 1253–1265, 1972

Dr. Reinhard Schepers
Institut für Geophysik
der Ruhr-Universität Bochum
D-4630 Bochum
Postfach 2148
Federal Republic of Germany